

Electronic Transport Switching by Electric field Driven Tautomerism in Single and Fused Metal-free Benziporphyrins

Yenni Ortiz-Acero¹, Arnau Cortés-Llamas¹, Jordi Ribas-Arino¹, Stefan T. Bromley^{1,2}

¹*Departament de Ciència de Materials i Química Física & Institut de Química Teòrica i Computacional (IQTCUB), Universitat de Barcelona, c/Martí i Franquès 1-11, 08028 Barcelona, Spain*

²*Institució Catalana de Recerca i Estudis Avançats (ICREA), Passeig Lluís Companys 23, 08010 Barcelona, Spain*

Abstract

The capacity of many metal-free porphyrins (MFPs) to exhibit different H-bonded tautomers provides a platform for exploring the effects of reversible molecular changes on electronic transport. On-surface and molecular junction experiments have shown that tautomerism in single MFPs can be controlled by the magnitude of the current passing through them. Such conductance-based results confirm the potential for tautomeric switching but are not easily translated into device applications, where faster electric field (E-field) gated switching is generally preferred. Previous work has focused on highly symmetric MFPs with a ring of four identical pyrrole rings, in which tautomers correspond to different H-N configurations of two protons. Herein, we consider a synthesized metal-free benziporphyrin in which one of the pyrrole rings is replaced with a phenol moiety. This modification lowers the symmetry of the system which leads to an increased tautomer-dependence of the electronic state. The structural anisotropy of benziporphyrins also has the potential to increase their selective switching responsive to applied E-fields. Here, use density functional theory and quantum electron transport calculations to assess: i) the statistical distribution of three distinct benziporphyrin tautomers with respect to different applied E-fields, and ii) the transport characteristics of each tautomer. We find that moderate E-fields can influence the tautomerism and that each tautomer has distinct transport characteristics, confirming that single metal-free beniporphyrins have potential to act as three-state molecular switches. By fusing two beniporphyrins, we show that the increased number of possible tautomeric states all retain their own distinct transport signature, thus opening the door to multi-state molecular registers. Finally, we show that fused beniporphyrins can also act as molecular wires in which transport can be enhanced with respect to a single beniporphyrin.

Introduction

Porphyrins are stable molecules based on a symmetric ring of four pyrrole units interconnected by methine bridges. Their ease of functionalisation and capacity to accommodate various metal ions allow for a precise manipulation of their electronic and chemical properties [1, 2]. Fused metal-containing porphyrins, for example, have been shown to sustain quantum coherence over considerable distances, making them ideal candidates for molecular level wires and transistors [3, 4]. Single and fused metal-free porphyrins (MFPs) have also attracted attention due to their π -electron magnetism with potential applications molecular spintronics [5, 6]. Most MFPs host two protons which can be exchanged between the nitrogen centres on the four pyrrole rings, giving rise to different tautomers. MFP-based tautomerization has attracted considerable attention as a potential platform for molecular switching [7, 8, 9, 10]. Tautomeric switching in MFPs is attractive for device applications as it: i) provides well-defined distinct molecular-based states, ii) is reversible, and iii) does not lead to significant structural changes to the MFP molecular skeleton.

To provide a useful switch, the tautomers in MFPs should be accessible through external stimuli. Such control of MFP tautomerism was first demonstrated by varying the current through single MFPs absorbed on a surface [7]. Conductance-based MFP-tautomerism has also been reported in single molecular junction experiments [10]. These experiments, along with theoretical studies [8], clearly show that the different tautomers have distinct electronic transport properties. For device applications, control of tautomerism by electric field (E-field) gating is desirable. Using a scanning tunneling microscope tip to address surface-bound MFPs, it has also been shown that the barrier for tautomerism can be lowered by applied E-fields [9]. However, thus far, selective control of tautomerism by applied E-fields in MFPs has not been achieved. One potential limitation of MFPs for E-field switching is their highly symmetric structure which means that different tautomers have low, or even zero dipole moments hindering effective coupling to external applied E-fields. To investigate more asymmetric tautomerism in a MFP-based approach, we consider metal-free benziporphyrins (MFBPs). MFBPs break the symmetry of MFPs by replacing one five -membered pyrrole ring by a six-membered benzenoid ring [11, 12]. MFBPs can thus host an increased range of structurally and energetically distinct tautomers.

Herein we consider an experimentally synthesized MFBP in which at least three distinct tautomers have been observed. We use density functional theory (DFT) and nonequilibrium Green's function (NEGF) calculations to explore the how externally applied E-fields can help select specific tautomers, and the associated changes in their transport properties. We first show that suitably oriented E-fields with experimentally realizable magnitudes can provide a strong energetic bias for selecting between three MFBP tautomers. We then consider single molecular junctions for the three MFBP tautomers, and

junctions of two fused MFBP with six different combinations of the corresponding three tautomers. In all junctions we find one or two step-wise jumps in current with respect to increases in bias voltage. The magnitude and voltage-dependence of these jumps are specific to each junction showing that each individual tautomer and combinations thereof would have a distinct and measurable transport signature. Taken together, these results demonstrate the potential of MFBPs as E-field gateable multistate molecular device components. By modifying the chemical links between the MFBPs and the junction contacts, we further show how this discrete multistate behaviour can be transformed into a more gradual current versus voltage response characteristic of a molecular wire. In these systems we also observe enhanced coherent transport. Overall, our study highlights MFBPs as novel and versatile E-field responsive building blocks for molecular electronics.

Methodology

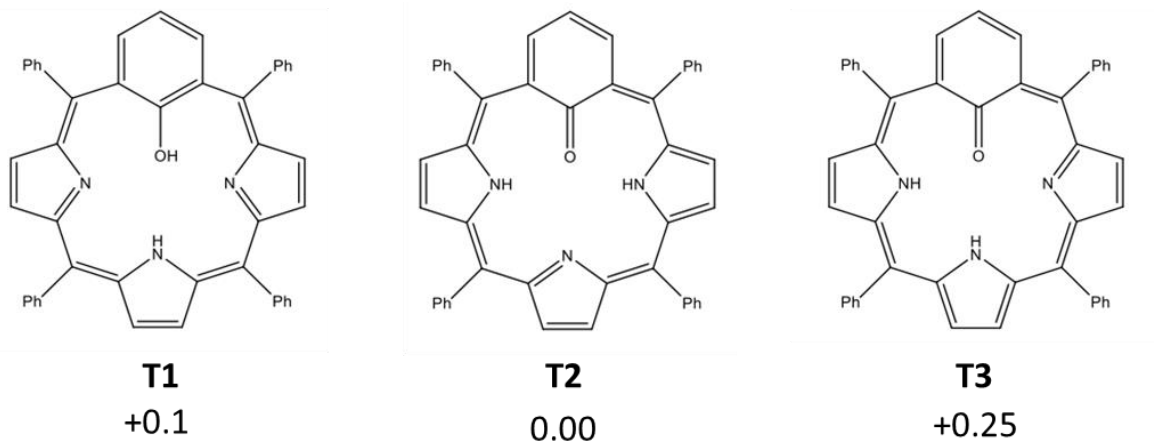


Figure 1. Chemical structures of the three considered benzoporphyrin tautomers: **T1**, **T2** and **T3**. Relative DFT-calculated total energies for zero applied E-field are given in eV with respect to **T2**.

We consider the experimentally synthesized 22-Hydroxybenzoporphyrin MFBP which contains a phenol moiety [13]. This MFBP has exists as an equilibrium mixture of two distinct tautomers which rapidly interchange. We consider these two tautomers (T1 and T2) and a third slightly higher energy tautomer (T3). Using DFT calculations we first established that each of these three tautomers corresponds to a well-defined distinct energy minimum and all are close in energy (see figure 1). We note that the in-plane dipole moments of these tautomers is strongly dependent on the in-plane axis and for any fixed axis it can vary over two Debyes between tautomers (see Suppl.

Info.). These three tautomers were then modelled with respect to their response to E-fields and their electronic transport properties.

Influence of applied E-fields on tautomerization

Relaxed structures of all molecular diradicals were obtained via density functional theory (DFT) based optimisations using the PBE0 hybrid exchange-correlation functional [14], and a 6-311g(d,p) basis set, as implemented in the Gaussian09 [15] code. Dispersion interactions were included using Grimme's D3 scheme [16,17]. Applied E-field were included via the "Field" keyword to define the direction and strength of an applied uniform E-field. In such calculations, a new term accounting for the potential due to the E-field is added to the external potential of the Kohn-Sham Hamiltonian. The Kohn-Sham equations are then solved taking into account the effective potential and thus the relaxation of the electronic density is self-consistently evaluated with influence of the applied E-field. Uniform E-fields were thus applied to all tautomers in two in-plane directions (i.e. with respect to the plane defined by the three N atoms of each tautomer) with field strengths ranging from zero to 0.5 V/Å. To assess the influence of the applied E-field, we evaluated the fractional populations of each T_n tautomer ($P(n)$) for all field strengths and both field directions

$$P(n) = \frac{1}{Z} e^{\frac{-E_n}{k_B T}} \quad (1)$$

where E_n is the relative total energy of each tautomer n , T is the temperature (assumed to be standard temperature, 273.15 K), Z is the total partition function for all three tautomers, and k_B is the Boltzmann constant.

Quantum electron transport calculations

Quantum electron transport calculations employed model junctions in which the MFBPs were connected between two gold clusters via sulfur atoms (see structures of specific junction set-ups below). We employed gold clusters composed of 19 atoms in a face-centered cubic structure cut from the bulk crystal structure. DFT calculations using the B3LYP exchange-correlation functional [] together with the LANL2DZ basis set were employed to treat this junction region. LANL2DZ combines effective core potentials (ECPs) with double-zeta quality basis functions for the valence electrons of the Au atoms, with an explicit all-

electron basis set for the lighter elements of the MFBPs. The double-zeta basis set is adequate for achieving qualitative accuracy and is specifically employed to mitigate ghost transmission issues [18]. This choice allows for a reliable representation of the electronic structure while minimizing artifacts that can arise in transport calculations. The explicitly represented Au contacts were coupled to virtual semi-infinite leads, to allow for the electron transport through the system to be calculated by means of the nonequilibrium Green's function method (NEGF) [19, 20, 21] as implemented in the ARTAOS software package [22]. In the NEGF calculations the Green's function of the scattering region $G(E)$ is evaluated following equation 2.

$$G(E) = (E S - H - \Sigma_S - \Sigma_D)^{-1} \quad (2)$$

where E represents the electron energy, H denotes the effective single-particle Kohn-Sham Hamiltonian, and S is the overlap matrix obtained from the DFT optimization. The self-energies $\Sigma_{S/D}$ account for the influence of the source and drain reservoirs, which are coupled to the system via the gold clusters to facilitate electron injection and extraction. These reservoirs are modeled using the wideband approximation [23]. With the Green's function, the transmission function can be calculated as

$$T(E) = 4\text{Tr}[\text{Im}(\Sigma_S)G\text{Im}(\Sigma_D)G^\dagger] \quad (3)$$

as well as the local transmissions between atoms i and j

$$T_{ij}(E) = \text{Im}(H_{ij}^* G_{ij}^n) \quad (4)$$

where the correlation function is given by

$$G^n = 2G \text{Im}(\Sigma_S)G^\dagger \quad (5)$$

The current is determined by integrating the energy-dependent transmission function T . The range of integration depends on the equilibrium Fermi energy E_F of the electrodes and the applied bias voltage.

$$I(V) = \frac{2e}{h} \int_{E_F - \frac{eV}{2}}^{E_F + \frac{eV}{2}} dE T(E, V) \quad (6)$$

where e is the unit electronic charge and h is Plank's constant.

Results and Discussion

In figure 2 we show how the fractional populations of each tautomer varies with respect to applied E-field strength for two indicated in-plane E-field directions. We consider a range of field strength from zero to $1 \text{ V}/\text{\AA}$. We note that such E-field strengths are achievable with devices based on dual ionic liquid gating that can generate up to $0.4 \text{ V}/\text{\AA}$,²⁴ or via STM tips which can generate E-fields up to $2.0 \text{ V}/\text{\AA}$.²⁵

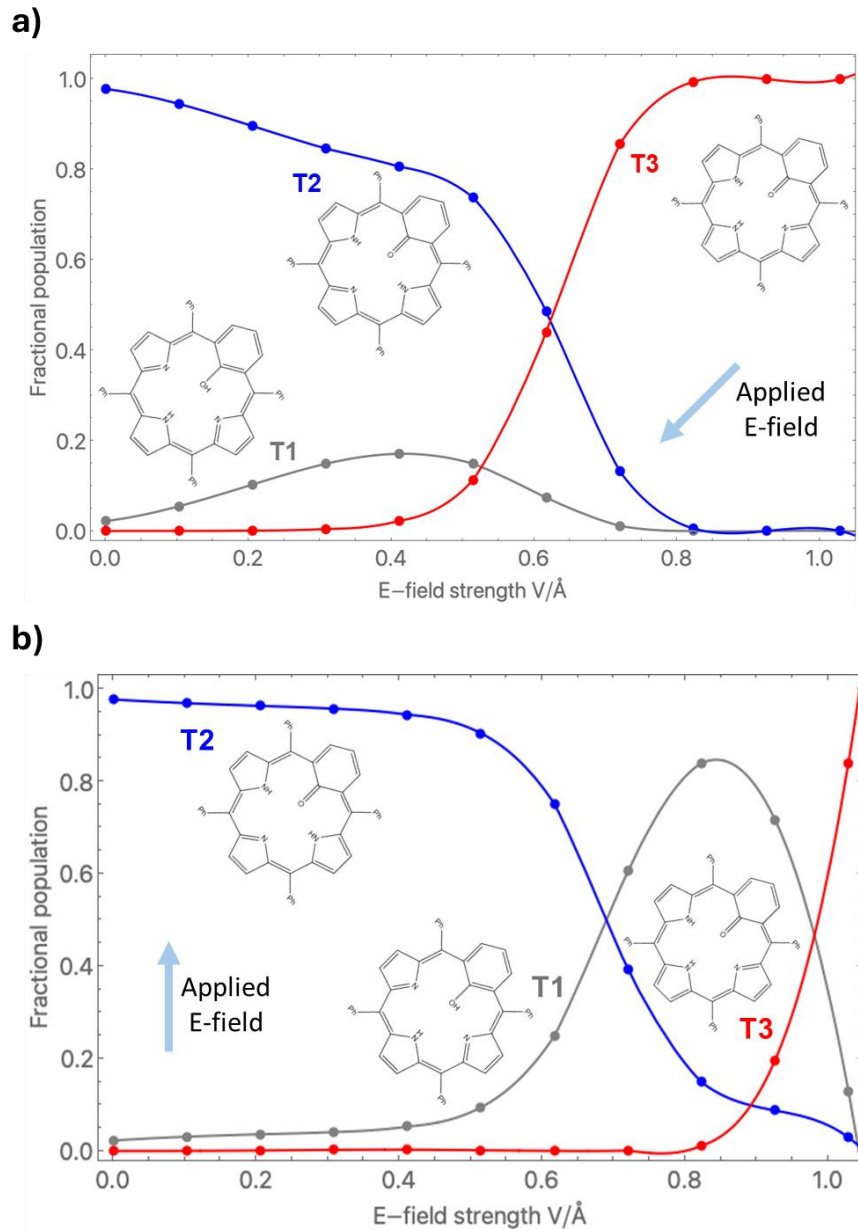


Figure 2. Graphic representing the fractional populations for each tautomer at 273.15 K with respect to the applied E-field strength for two field directions: a) 0° , and b) 225° .

For low E-field strengths for both considered field directions T2 is the dominant tautomer, as expected from its relatively high zero field stability (see Fig. 1). For the 225° E-field direction (see Fig. 2a) we observe a small gradual decrease of the dominance of T2 with increasing field strength up to 0.4 V/Å due to a small increase in the fraction of T1. For E-fields above 0.4 V/Å the prevalence of T1 falls away while T3 starts to strongly compete with T2. At an E-field strength of ~0.63 V/Å there is a crossover between T2 and T3 such that T3 becomes the dominant tautomer. In the 0° E-field direction case (Fig. 2b), we see a similar scenario to the 225° field direction for smaller fields, where the main competition is between T2 and a minor fraction of T1. Here, however, the increase in the fraction of T1 is much stronger such that the T1 begins to dominate over T2 at an E-field strength of ~0.69 V/Å. For even larger fields the T3 tautomer eventually becomes dominant again. We note that for all tautomers the applied E-field causes only very minor structural distortions to the MFBP skeleton indicating that the E-field-induced proton transfer would be an efficient process.

E-field gated molecular switching

We first consider transport through junctions based on single tautomers (J_{Tn}) connected to the gold electrodes through two opposing pendant aryl rings (see example in Fig. 3a). The calculated current versus voltage curves (Fig. 3b) in each case show a single step-like increase in current at a specific bias voltage which then plateaus afterwards. The voltages at which these junction-specific current increases occur correspond to the maximum transmission energy, which is found to correspond to the energy of the highest occupied molecular orbital (HOMO) of the system in each case (see Fig. 3c). This is consistent with a transport regime dominated by coherent, molecule-centered transport. Of the three junctions, J_{T1} clearly has the highest current carrying capacity for the considered bias voltages. Local current analysis (see Fig. 3c) reveals that J_{T1} exhibits the most direct conduction pathway, with minimal branching of electron flow. This indicates that charge transport in J_{T1} proceeds predominantly along a single conjugated route connecting the electrodes, reducing scattering and destructive interference. In contrast, the more bifurcated current pathways in J_{T2} and J_{T3} display lower overall conductance, reflecting the impact of competing routes and partial current cancellation within the molecular framework.

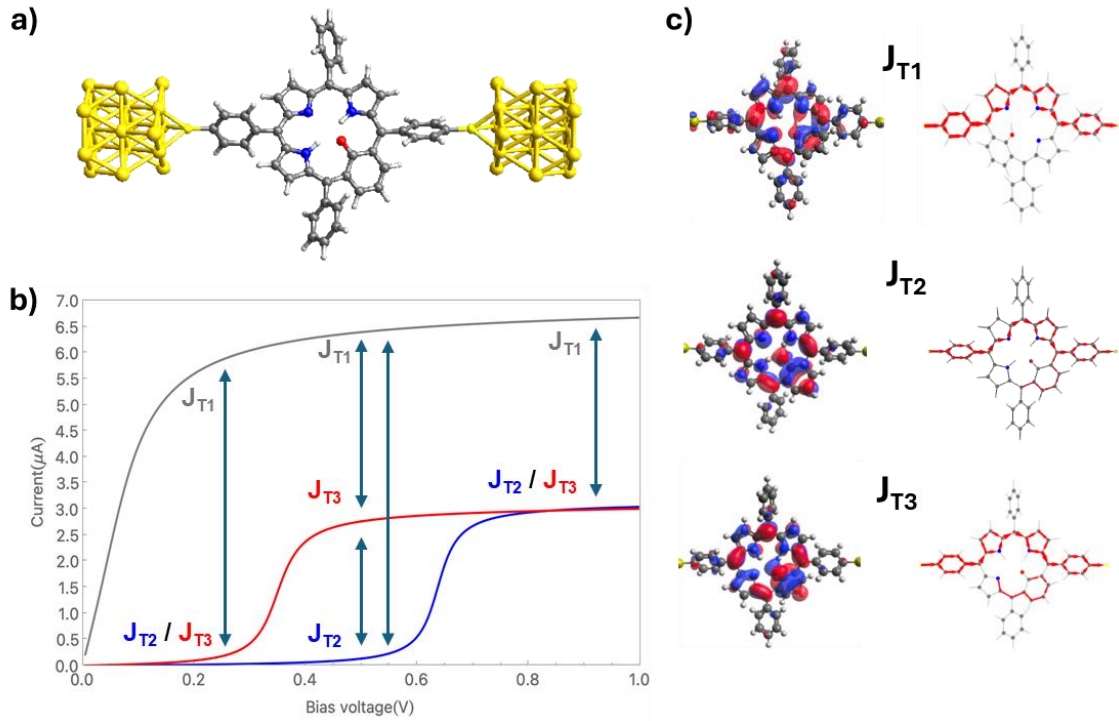


Figure 3. a) Structure of molecular junction model with the T1 MFBP tautomer linked to two gold electrodes via sulphur atoms (J_{T1}). Atom colour key: C – dark grey, O – red, N - blue, H - light grey, S - light yellow, Au - dark yellow. b) Calculated current with respect to bias voltage for three single MFBP junctions for three tautomers: T1 (J_{T1} - grey line), T2 (J_{T2} - blue line) and T3 (J_{T3} - red line). Reversible arrows indicate possible E-field induced tautomeric population shifts following figure 1. c) HOMO orbitals associated with the maximal transmission in each junction (left) and the corresponding transport pathways (right).

For the fused tautomers, we have calculated the current through all the six possible combinations between two tautomers from T1, T2 and T3 (see Supp. Info. for structural models) from which we observed well-defined characteristic current *vs* voltage responses as for the single tautomer junctions (see Fig. 4). These results suggest the potential for these systems as multi-state molecular devices [26, 27, 28]. Such systems extend beyond switchable two state ON/OFF systems and provide multiple stable configurations for enabling more complex information processing and enhanced data storage capacity.

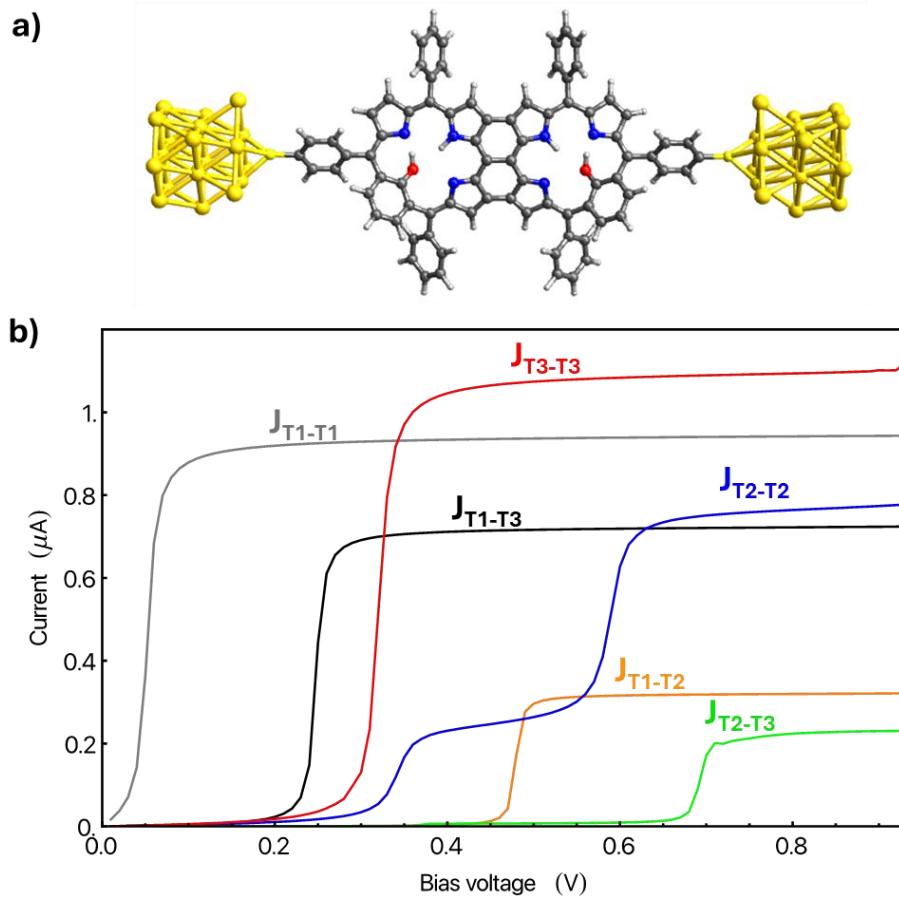


Figure 4. a) Structure of molecular junction model with the two fused T1 MFBP tautomers linked to two gold electrodes via sulphur atoms (J_{T1-T1}). Atom colour key follows that in figure 1. b) Calculated current with respect to bias voltage for six junctions comprised of fused combinations of T1, T2, T3 tautomers.

Influence of MFBP-Au linkers

The transport characteristics of a molecular junction can be strongly influenced by the way the molecule is functionalized and how it is linked to the electrodes. Here, we examine these effects in three different variants of J_{T2} (see Fig. 5), referred to as I, II and III. Case III is taken to be the junction shown in Fig. 2a. In case II, we remove with two pendant aryl rings. In case I, we replace the aryl rings linking the molecule with the electrodes with acetylenic linkers. See Fig. 5a for the structure of each junction variant.

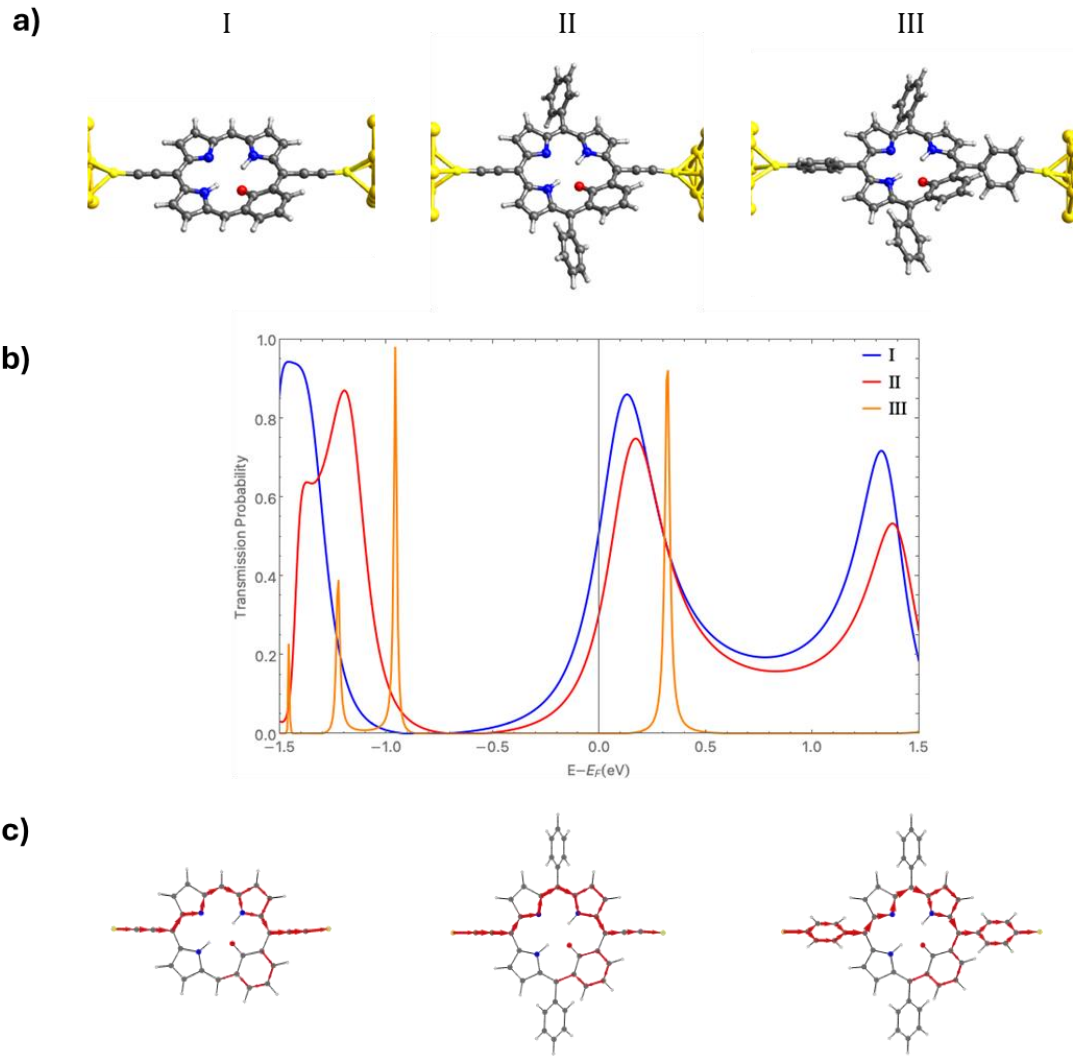


Figure 5. Comparison of the three variants of J_{T2} : Cases: I no aryl ring decoration and acetylenic electrode linkers, II with aryl ring decoration and acetylenic, and III aryl ring decoration and electrode linkers. For each case we show: a) structures, b) transmission functions, and c) local transport currents.

Comparing the transmission functions of cases I and II, we observe similar behavior of the transmission function. However, for the case III, a significant change in the transmission function was observed. These results are in line with studies showing the importance of the connection clusters in junctions [29]. Recent experimental conductance measurements of metal-containing porphyrin systems have also underscored the role of selecting appropriate electrode anchors for enhancing transmission [30]. Local transport analysis (see Fig. 5c) shows that the preferred current pathway in each of the three cases bypasses the benzene ring attached to the oxygen. This makes the deviation of this ring from the plane less impactful compared to the anchoring benzene rings.

MFBP molecular wires

Fused porphyrin oligomers are known as excellent molecular wires due to their efficient π -overlap, stability, rigid frameworks, and low reorganization energies [31]. Recent studies [30] have demonstrated that edge-fused porphyrins, composed of up to three porphyrin subunits connected to gold via thiolate groups, show rapidly narrowing HOMO–LUMO gap as the chain length increases, countering the effect of longer tunneling distances causing conductance to increase with length. This intriguing phenomenon has been observed in only a few systems.

As a minimal models of MFBP molecular wires we consider variants of J_{T1-T1} , J_{T2-T2} and J_{T3-T3} junctions in which we employ acetylenic linkers to the gold electrodes instead of aryl rings. In figure 6 we compare the current versus voltage characteristics of these junctions with those of their single molecule equivalents. In all cases the fused MFBP wires show a more complex pattern of increasing current with respect to bias voltage as compared to the single molecular junctions. While the current of in the single molecule systems tends to start levelling off at around 0.5 V, the current in the wire-like systems keeps increasing and eventually surpasses that of the former for voltages above approximately 1.5 V. This increase of current with increase in the number of MFBP units suggests that ballistic transport may be active in these systems. In a future work we plan to extend these studies to larger chains of fused MFBPs.

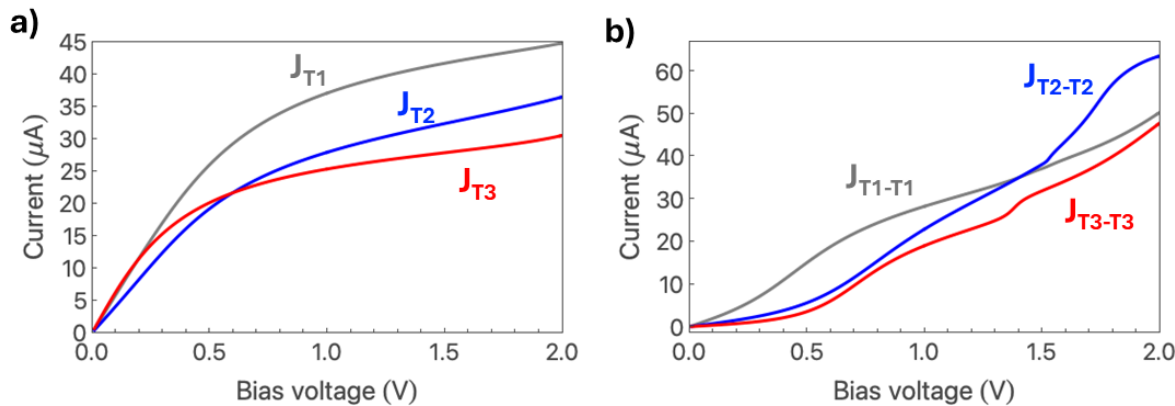


Figure 6. Current versus bias voltage plots for: a) J_{T1} , J_{T2} , and J_{T3} with acetylenic electrode linkers, b) J_{T1-T1} , J_{T2-T2} and J_{T3-T3} with acetylenic electrode linkers.

Conclusions

Our calculations have demonstrated that E-fields are able to bias tautomerization in asymmetric MFBPs. Specifically, we show that experimentally realizable E-fields could effectively select between three distinct isomers in an experimentally synthesized MFBP. We further show that each of these three tautomers displays a characteristic electron transport signature in molecular junctions, thus providing a measurable way to detect the tautomeric states. Fusing MFBPs provides a means to increase the number of distinct transport signatures, opening the door to multi-state molecular devices. By changing the way in which these fused MFBP systems link to the electrodes we can also access molecular wire-like transport where we observe surprisingly high current carry capacities. Overall, our work highlights how MFBPs could provide a new versatile platform for advancing single molecular devices and molecular based electronics.

Acknowledgements

The authors acknowledge the financial support from the Spanish Ministerio de Ciencia, Innovación y Universidades and Agencia Estatal de Investigación (AEI) MCIN/AEI/10.13039/501100011033 through projects PID2023-149691NB-I00, PID2021-127957NB-I00, TED2021-132550B-C21, PID2020-117803GB-I00), Spanish Structures of Excellence María de Maeztu program (CEX2021-001202-M), and Agència de Gestió d'Ajuts Universitaris i de Recerca of Generalitat de Catalunya (2021SGR00354 and 2023CLIMA00064).

References

- 1 Hiroto, S., Miyake, Y., Shinokubo, H., Synthesis and Functionalization of Porphyrins through Organometallic Methodologies, *Chem. Rev.*, 117, 4, 2910–3043 (2017).
- 2 Jurow, M., Schuckman A. E., Batteas J. D., Drain, C. M., Porphyrins as molecular electronic components of functional devices, *Coord. Chem. Rev.*, 254, 19–20 (2010).
- 3 Sedghi, G., García-Suárez, V., Esdaile, L. *et al.* Long-range electron tunnelling in oligo-porphyrin molecular wires. *Nature Nanotech* 6, 517–523 (2011).
- 4 Chen, Z., Deng, J., Hou, S., Bian, X., Swett, J., Wu, Q., Baugh, J., Bogani, L., Briggs, G., Mol, J., Lambert, C., Anderson, H., & Thomas, J., Phase-Coherent Charge Transport through a Porphyrin Nanoribbon. *Journal of the American Chemical Society*, 145, 15265 - 15274. (2022)
- 5 Zhao, Y., Jiang, K., Li, C. *et al.* Quantum nanomagnets in on-surface metal-free porphyrin chains. *Nat. Chem.* 15, 53–60 (2023).

6 Yan Zhao, Kaiyue Jiang, Can Li, Yufeng Liu, Chengyang Xu, Wanna Zheng, Dandan Guan, Yaoyi Li, Hao Zheng, Canhua Liu, Weidong Luo, Jinfeng Jia, Xiaodong Zhuang, and Shiyong Wang. Precise Control of π -Electron Magnetism in Metal-Free Porphyrins *J. Am. Chem. Soc.* 2020, 142, 43, 18532–18540.

7 P. Liljeroth, J. Repp, and G. Meyer Current-Induced Hydrogen Tautomerization and Conductance Switching of Naphthalocyanine Molecules. *Science* **317**, 1203 (2007).

8 J. Prasongkit, A. Grigoriev, and R. Ahuja. Interference effects in phtalocyanine controlled by H-H tautomerization: Potential two-terminal unimolecular electronic switch. *Phys. Rev. B* **84**, 165437 (2011).

9 Shai Mangel, Maxim Skripnik, Katharina Polyudov, Christian Dette, Tobias Wollandt, Paul Punke, Dongzhe Li, Roberto Urcuyo Fabian Pauly, Soon Jung Jung and Klaus Kern. Electric-field control of single-molecule tautomerization. *Phys. Chem. Chem. Phys.*, **22**, 6370 (2020).

10 Yan Z, Li X, Li Y, Jia C, Xin N, Li P, Meng L, Zhang M, Chen L, Yang J, Wang R, Guo X. Single-molecule field effect and conductance switching driven by electric field and proton transfer. *Sci Adv.* 2022 Mar 25;8(12) (2022).

11 Stepień, M., Latos-Grażyńska, L. Benziporphyrins: Exploring Arene Chemistry in a Macroyclic Environment, *Acc. Chem. Res.* **38**, 88-98 (2005).

12 Lash, T. D. Benziporphyrins, a unique platform for exploring the aromatic characteristics of porphyrinoid systems, *Org. Biomol. Chem.*, **13**, 7846 (2015).

13 Stepień, M., Latos-Grażyńska, L., Szterenberg, L., 22-Hydroxybenziporphyrin: Switching of Antiaromaticity by Phenol-Keto Tautomerization *J. Org. Chem.* **72**, 2259-2270 (2007).

14 Adamo, C., Barone, V. Toward reliable density functional methods without adjustable parameters: The PBE0 model, *J. Chem. Phys.*, **110**, 6158–6170 (1999).

15 Frisch, M.J. *et al. Gaussian 09, Revision D.01*, Gaussian, Inc., Wallingford CT, 2013

16 Grimme, S.; Antony, J.; Ehrlich, S.; Krieg, H. A consistent and accurate ab initio parametrization of density functional dispersion correction (DFT-D) for the 94 elements H-Pu. *J. Chem. Phys.* **132**, 154104 (2010).

17 Grimme, S.; Ehrlich, S.; Goerigk, L. Effect of the damping function in dispersion corrected density functional theory. *J. Comput. Chem.* **32**, 1456– 1465 (2011).

18 C. Herrmann, G. C. Solomon, J. E. Subotnik, V. Mujica, M. A. Ratner. Ghost transmission: How large basis sets can make electron transport calculations worse. *J. Chem. Phys.* **132**, 024103 (2010).

19 Supriyo Datta, Nanoscale device modeling: the Green's function method. *Superlattices and Microstructures*, **28**, 4 (2000).

20 Camsari, K.Y., Chowdhury, S., Datta, S. The Nonequilibrium Green Function (NEGF) Method. In: Rudan, M., Brunetti, R., Reggiani, S., Springer Handbook of Semiconductor Devices

21 Gao, F., Menchón, R.E., Garcia-Lekue, A., Brandbyge, M. Tunable spin and conductance in porphyrin-graphene nanoribbon hybrids. *Commun Phys* **6**, 115 (2023).

22 M. Deffner, L. Groß, T. Steenbock, B. A. Voigt, G. C. Solomon, and C. Herrmann, ARTAIOS, a code for postprocessing quantum chemical electronic structure calculations, <https://www.chemie.uni-hamburg.de/institute/ac/arbetsgruppen/herrmann/software/artaios.html>

23 C. J. O. Verzijl, J. S. Seldenthuis, and J. M. Thijssen. Applicability of the wide-band limit in DFT-based molecular transport calculations. *J. Chem. Phys.* **138**, 094102 (2013).

24 Weintrub, B. I.; Hsieh, Y.-L.; Kovalchuk, S.; Kirchhof, J. N.; Greben, K.; Bolotin, K. I. Generating intense electric field in 2D materials by dual ionic gating. *Nat. Commun.*, **13**, 6601 (2002).

25 Alemani, M.; Peters, M. V.; Hecht, S.; Rieder, K.-H.; Moresco, F.; Grill, L. E-field-Induced Isomerization of Azobenzene by STM. *J. Am. Chem. Soc.*, **128**, 14446–14447 (2006).

26 Jialing Li, Bo-Ji Peng , Shi Li, Daniel P. Tabor , Lei Fang. Charles M. Schroeder Ladder-type conjugated molecules as robust multi-state single-molecule switches, *Chem* **9** 2282-2297 (2023).

27 B. Sun, S. Ranjan, G. Zhou, T. Guo, Y. Xia, L. Wei, Y.N. Zhou, Y.A. Wu. Multistate resistive switching behaviors for neuromorphic computing in memristor. *Materials Today Advances*, **9**, 100125 (2021).

28 Changqing Ye, Qian Peng, Mingzhu Li, Jia Luo, Zhengming Tang, Jian Pei, Jianming Chen, Zhigang Shuai, Lei Jiang, and Yanlin Song, Multilevel conductance switching of memory device through photoelectric effect, *J. Am. Chem. Soc.*, **134**, 49 (2012).

29 Abraham Nitzan, and Mark A. Ratner. Electron Transport in Molecular Wire Junctions. *Science* **300**, 1384-1389 (2003).

30 Jie-Ren Deng, M. Teresa González, He Zhu, Harry L. Anderson, and Edmund Leary. Ballistic Conductance through Porphyrin Nanoribbons. *Journal of the American Chemical Society*, **146** (6), 3651-3659 (2024)

31 Zwick, P.; Dulić, D.; van der Zant, H. S. J.; Mayor, M. Porphyrins as building blocks for single-molecule devices. *Nanoscale*, **13**, 15500–15525 (2021).